

Photoluminescence from SiO₂ films containing Si nanocrystals and Er: Effects of nanocrystalline size on the photoluminescence efficiency of Er³⁺

Minoru Fujii^{a)}

Department of Electrical and Electronics Engineering, Faculty of Engineering, Kobe University, Rokkodai, Nada, Kobe 657-8501, Japan

Masato Yoshida

Division of Electrical and Electronics Engineering, The Graduate School of Science and Technology, Kobe University, Rokkodai, Nada, Kobe 657-8501, Japan

Shinji Hayashi and Keiichi Yamamoto

Department of Electrical and Electronics Engineering, Faculty of Engineering, Kobe University, Rokkodai, Nada, Kobe 657-8501, Japan

(Received 23 February 1998; accepted for publication 20 July 1998)

SiO₂ films containing Si nanocrystals (nc-Si) and Er were prepared and their photoluminescence (PL) properties were studied. The samples exhibited PL peaks at 0.8 and 1.54 μm, which could be assigned to the electron-hole recombination in nc-Si and the intra-4*f* transition in Er³⁺, respectively. Correlation between the intensities of the two PL peaks was studied as functions of the size of nc-Si, Er concentration, excitation power and excitation wavelength. It was found that the 1.54 μm PL of Er³⁺ is strongly enhanced by incorporating nc-Si in films. Furthermore, the intensity of the 1.54 μm peak was found to depend strongly on the size of the incorporated nc-Si. © 1998 American Institute of Physics. [S0021-8979(98)06320-8]

I. INTRODUCTION

Recently, Er-doped Si has been attracting much interest because of its potential application in Si-based optoelectronic devices. The Er³⁺ ions incorporated into Si produce light emission from the intra-4*f* transition (⁴I_{13/2}-⁴I_{15/2}) at around 1.54 μm, which corresponds to the absorption minimum in silica-based glass fibers.¹⁻⁵ Interest has also been focused on Er-doped porous Si, which emits strong 1.54 μm photoluminescence (PL) even at room temperature and exhibits very weak thermal quenching of the PL.⁵⁻⁹ Porous Si consists of nanometer-size Si crystals (nc-Si). In porous Si, excitation of Er³⁺ is considered to occur through the recombination of photogenerated carriers in the nc-Si and the subsequent energy transfer to Er³⁺.⁷⁻⁹

The electronic band structure of nc-Si, as small as several nanometers, is much different from that of the bulk-Si crystal due to the quantum confinement effects of electrons, holes and phonons (quantum size effects). The most prominent feature of the quantum confinement effects is the widening of the band gap from that of the bulk-Si crystal. The widening of the band gap is considered to result in the small thermal quenching of the PL observed for Er-doped porous Si.⁷⁻⁹ Since the electronic band structure of nc-Si depends strongly on the size, the efficiency of the 1.54 μm PL of Er³⁺ excited by the energy transfer from nc-Si may also depend strongly on the size of nc-Si.

As is well known, nc-Si as small as several nanometers in diameter emits light at the near-infrared and visible regions due to the band-to-band transition between the widened band gap.¹⁰⁻¹² If the Er³⁺ is excited by the energy

transfer from nc-Si, the 1.54 μm PL of Er³⁺ and the visible or near-infrared PL of nc-Si are considered to correlate to each other depending on the size of nc-Si, number of active Er³⁺ ions and excitation energy and power. Detailed studies of these dependences will give deeper insight into the nc-Si mediated excitation mechanism of Er³⁺.

To study these dependences of the two PL bands, stable nc-Si with well-defined size and shape as well as chemical composition is indispensable. For this purpose, porous Si is not appropriate because of its instability, complexity in its structure and chemical composition, and resulting ambiguity in the origin of the PL. Instead of porous Si, in our previous work, we employed SiO₂ films containing nc-Si (Refs. 10, 13, and 14) as a host of Er³⁺ and studied the PL properties as a function of Er concentration.¹⁵ For the samples containing both nc-Si and Er, two PL peaks corresponding to the recombination of electron-hole pairs in nc-Si and the intra-4*f* transition in Er³⁺ could be observed simultaneously. From the correlation of the two PL peaks, we clearly demonstrated that the excitation of Er³⁺ is made by the energy transfer from nc-Si. This work is an extension of the previous work. In order to further clarify the nc-Si mediated excitation mechanism of Er³⁺, we performed systematic PL studies for SiO₂ films containing nc-Si and Er. In particular, we have studied in detail the effects of nanocrystalline size on the PL efficiency of Er³⁺. We will demonstrate that the intensity of the 1.54 μm PL of Er³⁺ is strongly enhanced by incorporating nc-Si in films, and that the PL intensity depends strongly on the size of nc-Si.

II. EXPERIMENT

Samples were prepared by a rf cosputtering method. In our previous studies,^{10,13,14,16} we demonstrated that nc-Si em-

^{a)}Electronic mail: fujii@eedept.kobe-u.ac.jp

bedded in SiO₂ films can be obtained by cosputtering Si and SiO₂ and postannealing at 1100 °C or higher. In this work, in an attempt to dope Er in the films, Er₂O₃ pellets were added as the sputtering targets.¹⁵ In actual sputtering procedures, small pieces of Si chips 5×15 mm² in size and Er₂O₃ pellets 10 mm in diameter were placed on a SiO₂ target (10 cm in diameter) and they were cosputtered. Films of about 1 μm in thickness were deposited onto fused quartz plates. After the deposition, the samples were annealed in an atmosphere of N₂ gas for 30 min at 1100 °C.

In this method, the size of nc-Si can be controlled by changing the number of Si chips during the cosputtering. Er concentration (C_{Er}) can also be controlled by changing the number of Er₂O₃ pellets during the cosputtering. The C_{Er} and the volume fraction of nc-Si in the films (f_{Si}) were determined by electron-probe microanalyses [using JCSA-733 (JEOL)]. The size of nc-Si was determined by cross-sectional high-resolution transmission electron microscopic (HRTEM) observations. An electron microscope [JEM-2010 (JEOL)] operated at 200 kV was used. In this work, we have studied the samples with C_{Er} ranging from 0 to 0.11 at. % and f_{Si} ranging from 7 to 21 vol. %. By varying f_{Si} from 7 to 21 vol. %, the average diameter of nc-Si (d_{Si}) was changed from 2.7 to 3.8 nm.

The PL spectra were measured using a HR-320 (Jobin-Yvon) monochromator and an EO-817L (North Coast) Ge detector. The excitation sources were six lines of an Ar-ion laser and a He-Ne laser with a power density of less than 1.5 W/cm². Spectral responses of the detection systems were corrected by reference spectra of a standard tungsten lamp. The temperature dependence of the PL spectra was measured from 15 to 300 K in a CF1204 continuous-flow He cryostat (Oxford).

III. RESULTS

A. HRTEM observation

Figure 1 shows a typical cross-sectional HRTEM image of the SiO₂ film containing nc-Si ($f_{\text{Si}}=11$ vol. %). We can clearly see lattice fringes in the image. The lattice fringes correspond to the {111} planes of Si crystals with the diamond structure. The crystallinity of the nanocrystals is rather good. The nanocrystals are not aggregated and are isolated in SiO₂ matrices. The average diameter of the nanocrystals estimated from the image was about 3.1 nm. It should be noted here that the size of nc-Si is almost independent of C_{Er} and depends only on f_{Si} for the samples with $C_{\text{Er}} \leq 0.11$ at. %. In the case of an Er-implanted SiO₂ film annealed at 1200 °C, precipitates of Er as large as several tens of nanometers have been observed in HRTEM observations.⁵ In the present samples, such large precipitates were not found in the HRTEM images. However, we cannot neglect the possibility that much smaller Er clusters exist in films, because Er clusters smaller than about 2 nm are considered to be not detectable by HRTEM observations due to the strong background images of SiO₂ matrices.

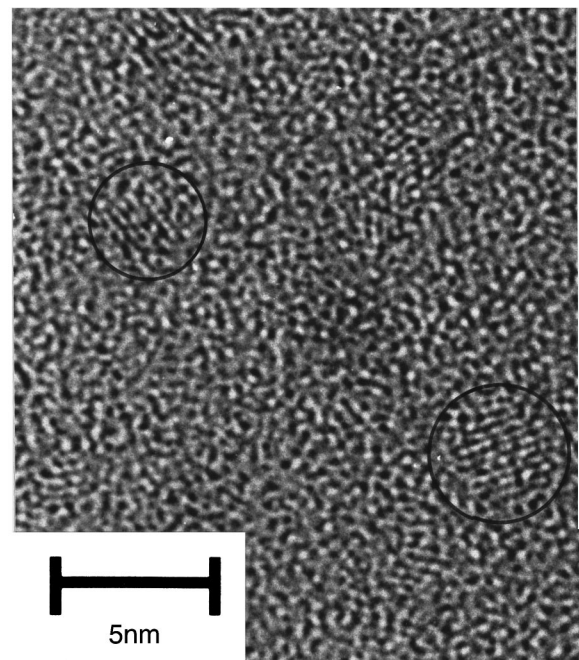


FIG. 1. Typical HRTEM image of SiO₂ films containing nc-Si ($f_{\text{Si}}=11$ vol. %). Lattice fringes corresponding to the {111} planes of Si can clearly be seen. The average diameter of the nanocrystals estimated from the image is about 3.1 nm.

B. Dependence of PL spectra on the size of nc-Si

Figure 2 shows the PL spectra of SiO₂ films containing nc-Si and Er as a function of f_{Si} (d_{Si}). The inset is an expansion of the region between 1.46 and 1.65 μm. The volume fraction of nc-Si (f_{Si}) was changed from 0 to 21 vol. %, while C_{Er} was fixed at about 0.04 at. %. As f_{Si} was changed from 7 to 21 vol. %, d_{Si} changed from 2.7 to 3.8 nm. The film thickness was fixed at about 1.2 μm. For the sample not containing nc-Si, we can see a very weak peak at about 1.54 μm, corresponding to the intra-4f transition of Er³⁺ (⁴I_{13/2}–⁴I_{15/2}).² By adding nc-Si to the films, the intensity of the 1.54 μm peak increases drastically. Although the intensity increases drastically by adding nc-Si, its dependence on f_{Si} is not simple. It was found that the intensity becomes maximum (about 200 times stronger than that of the sample not containing nc-Si) when $f_{\text{Si}} \approx 7$ vol. % ($d_{\text{Si}} \approx 2.7$ nm). By further increasing f_{Si} from 7 to 21 vol. %, i.e., by increasing d_{Si} from 2.7 to 3.8 nm, the PL intensity decreased rapidly.

In addition to the 1.54 μm peak, the samples containing nc-Si show a peak at about 0.8 μm. From our previous PL studies,¹⁰ the 0.8 μm peak can be assigned to the recombination of electron-hole pairs in nc-Si. In Fig. 2, we can see that the peak energy and the intensity of the 0.8 μm peak depend strongly on the size of nc-Si. As the size decreases, the peak becomes intense and shifts to higher energies. The high-energy shift is caused by the widening of the band gap due to the quantum size effects.¹⁰ The increase in the PL intensity is considered to be due to the increase in the oscillator strength,¹⁷ and/or the decrease in the nonradiative Auger recombination process.¹⁸

Figure 3 shows the intensities of the 1.54 and 0.8 μm peaks as a function of d_{Si} . The intensities are corrected by

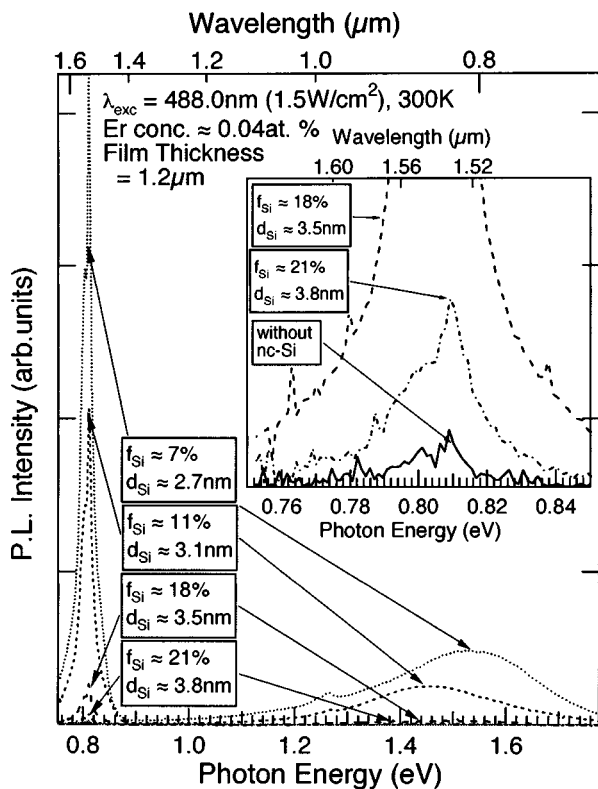


FIG. 2. PL spectra of SiO₂ films containing nc-Si and Er. The inset is an expansion of the region between 1.46 and 1.65 μm. The Er concentration and film thickness for all the samples are fixed at 0.04 at. % and 1.2 μm, respectively, and the concentration of the Si nanocrystals is varied from 0 to 21 vol. %.

the amount of nc-Si contained in the films by dividing the observed intensities by f_{Si} . For comparison purposes, the intensities are normalized at their maximum intensities obtained for $d_{Si} \approx 2.7$ nm. We can see that as d_{Si} decreases from 3.8 to 2.7 nm, the 0.8 μm peak of nc-Si becomes about

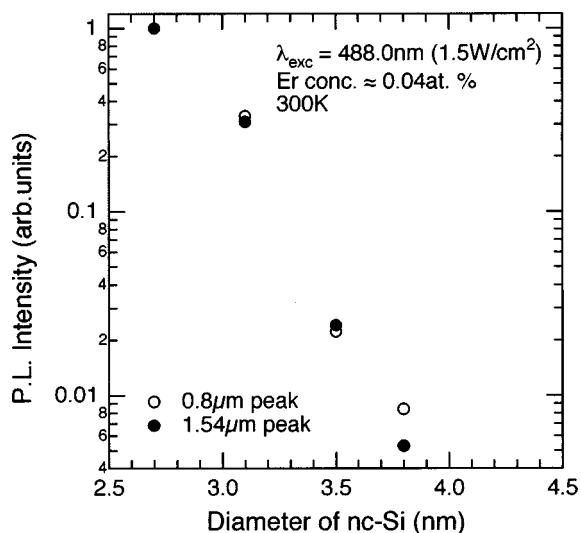


FIG. 3. PL intensities [(●) 1.54 μm peak, (○) 0.8 μm peak] as a function of the diameter of nc-Si. The intensities are corrected by the amount of nc-Si contained in the films by dividing the observed intensities by the Si concentration (f_{Si}). The intensities are normalized at their maximum intensities at $d_{Si} = 2.7$ nm for the comparison purposes.

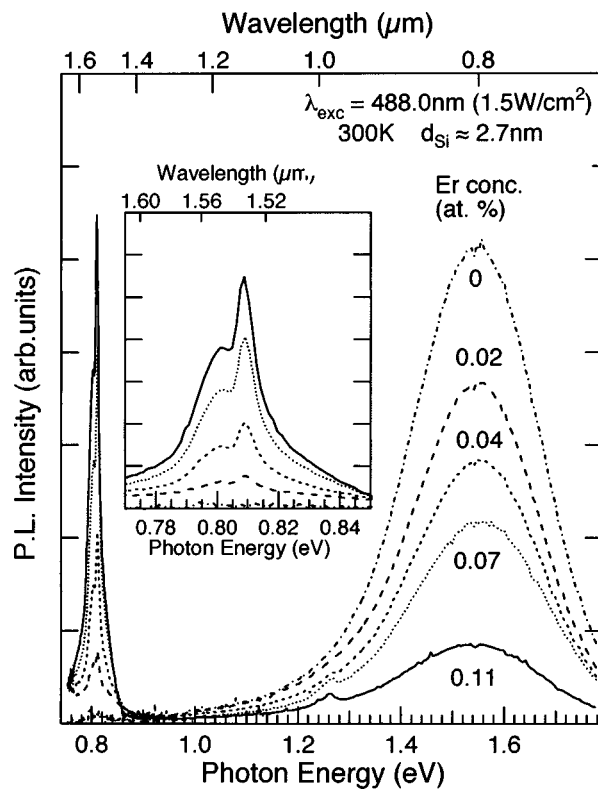


FIG. 4. PL spectra of SiO₂ films containing nc-Si and Er. The inset is an expansion of the region between 1.46 and 1.61 μm. The size of nc-Si is about 2.7 nm and the Er concentration is varied from 0 to 0.11 at. %.

two orders of magnitude more intense. At the same time, the 1.54 μm peak of Er³⁺ also becomes more intense depending on the size of nc-Si. It should be stressed here that the intensity of the 1.54 μm peak of Er³⁺ exhibits nearly the same size dependence as that of the 0.8 μm peak of nc-Si.

C. Dependence of PL spectra on the Er concentration

Figure 4 shows the dependence of PL spectra on C_{Er} . The size (volume fraction) of nc-Si is fixed at about 2.7 nm in diameter ($f_{Si} \approx 7$ vol. %). The inset is an expansion of the region between 1.46 and 1.61 μm. For the sample not containing Er, we can see a peak of nc-Si at about 0.8 μm. As C_{Er} increases, the intensity of the 0.8 μm peak decreases rapidly. It is noted that, in spite of the drastic change in the intensity, the peak energy is independent of C_{Er} . This suggests that the size of nc-Si is not affected by C_{Er} , because the peak energy is very sensitive to the size.¹⁰ In contrast to the 0.8 μm peak, the 1.54 μm peak of Er³⁺ becomes intense as C_{Er} increases. Figure 5 compares the intensities of the two peaks as a function of C_{Er} . We can see that the 1.54 μm peak becomes intense almost linearly with C_{Er} , while the 0.8 μm peak decreases rapidly.

D. Temperature dependence of the PL spectra

Figure 6 shows the temperature dependence of the PL spectra for the samples with $C_{Er} \approx 0.04$ at. % and $d_{Si} \approx 2.7$ nm. At room temperature, we can see peaks at about 1.54 and 0.8 μm. As the temperature decreases, the intensity of the 1.54 μm peak increases slightly, while that of the 0.8 μm

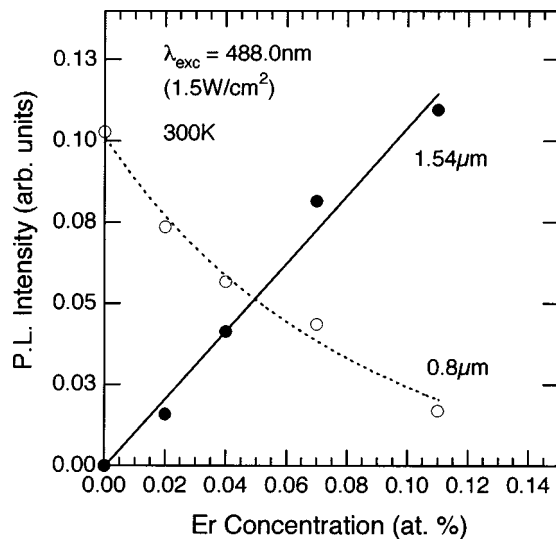


FIG. 5. PL intensities of 1.54 and 0.8 μm peaks as a function of Er concentration. The lines are drawn to guide the eye.

peak first increases and then decreases. In addition to these peaks, another peak appears at about 1.2 μm below 150 K. This peak becomes intense with decreasing temperature. The origin of the 1.2 μm peak is considered to be the recombination of carriers trapped at P_b centers at the interfaces between nc-Si and SiO_2 matrices.^{19,20} Figure 7 shows the intensity of the 1.54 μm peak as a function of a temperature. Although the intensity slightly decreases as the temperature

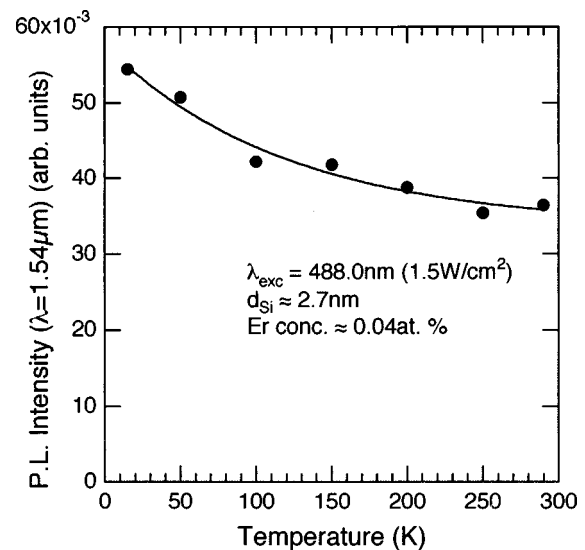


FIG. 7. The intensity of the 1.54 μm peak as a function of temperature. The line is drawn to guide the eye.

increases, the degree of thermal quenching is very small. The PL is quenched only about 30% from 15 to 290 K. This value is much smaller (about two orders of magnitude) than that reported for the Er-doped bulk-Si crystal.⁴ Similar very small thermal quenching has been observed for all the samples.

In Fig. 6, the energy of the 1.54 μm peak is almost independent of the temperature, while that of the 0.8 μm peak depends on the temperature. As the temperature decreases, the 0.8 μm peak shifts to higher energy. The degree of the high-energy shift was nearly the same as that of the band-gap of the bulk-Si crystal [about 45 meV (300 to 5 K)]. We have studied in detail the size and temperature dependence of the 0.8 and 1.2 μm peaks for the samples not containing Er. The results will be published elsewhere.

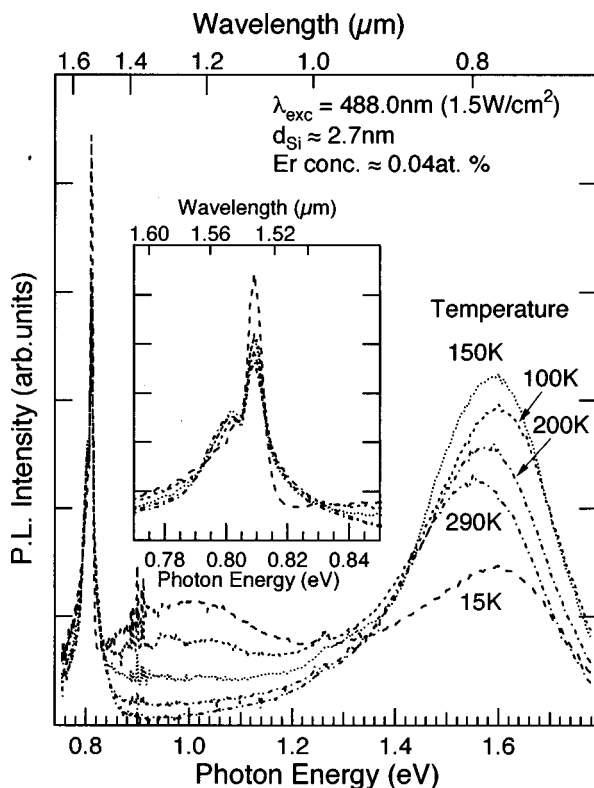


FIG. 6. Temperature dependence of the PL spectra of SiO_2 films containing nc-Si and Er. The size of nc-Si is about 2.7 nm and the Er concentration is about 0.04 at. %. The inset is an expansion of the region between 1.46 and 1.61 μm .

IV. DISCUSSION

As shown in Figs. 2 and 3, the intensity of the 1.54 μm peak of Er^{3+} is strongly enhanced by incorporating nc-Si into the films. Furthermore, the intensity of the 1.54 μm peak depends strongly on the size of nc-Si, and the size dependence is almost the same as that of the 0.8 μm peak of nc-Si, i.e., the intensity ratio of the 1.54 and 0.8 μm peaks is a constant independent of the size of nc-Si provided that C_{Er} is the same. The results of Figs. 2 and 3 suggest that much more intense 1.54 μm PL may be achieved by codoping much "brighter" nc-Si. Since the PL intensity of nc-Si becomes intense as the size decreases, PL study of the sample containing much smaller nc-Si (<2.7 nm) is promising in learning more.

In this work, we controlled d_{Si} by changing f_{Si} . As f_{Si} increases, an interaction between nc-Si may increase, and the interaction may affect the PL efficiency of Er^{3+} . Therefore, in order to study purely the size dependence, d_{Si} should be controlled without changing f_{Si} . Unfortunately, until now, we have not succeeded in controlling d_{Si} under fixed f_{Si} and thus cannot discuss the effects of the interactions in detail.

Although the intensity ratio of the 1.54 and 0.8 μm peaks does not depend on the size, it depends strongly on C_{Er} as can be seen in Figs. 4 and 5. The intensity of the 1.54 μm peak increases as C_{Er} increases, while the 0.8 μm peak decreases. By assuming an energy transfer from nc-Si to Er^{3+} , these results can be explained as follows. First, the excitation light is absorbed mainly by nc-Si and the electron-hole pairs are generated in the nanocrystals. A part of the recombination energy of the electron-hole pairs is then transferred to Er^{3+} . The amount of energy transferred to Er^{3+} increases as C_{Er} increases. This results in growth of the 1.54 μm peak and quenching of the 0.8 μm peak with increasing C_{Er} .

Since the intensity of the 1.54 μm peak in Fig. 5 depends nearly linearly on C_{Er} , the energy transfer from nc-Si to Er^{3+} is considered to be limited by the number of optically active Er^{3+} in the films (i.e., almost all optically active Er^{3+} ions are excited by the energy transfer). In this case, we can expect much different excitation power (P_{ex}) dependence for the Er^{3+} and nc-Si peaks. Since the amount of the energy transferred to Er^{3+} is limited by the number of Er^{3+} , the intensity of the 1.54 μm peak will not depend linearly on P_{ex} but will be saturated at rather low P_{ex} , while that of the 0.8 μm peak will not be saturated. The saturated intensity of the 1.54 μm peak will depend on C_{Er} .

Figure 8 shows the P_{ex} dependence of the intensities of 1.54 μm [Fig. 8(a)] and 0.8 μm [Fig. 8(b)] peaks for the samples with C_{Er} of 0.02 and 0.07 at. %. The average diameter of nc-Si is about 2.7 nm. For comparison purposes, the PL intensity of the sample not containing nc-Si and with C_{Er} of 0.07 at. % is also shown in Fig. 8(a). Since the PL intensity of the sample not containing nc-Si is very weak, the raw intensity is multiplied by a factor of 30. We can see that the 1.54 μm peak of the samples containing nc-Si exhibits very small P_{ex} dependence and is almost saturated [Fig. 8(a)], while that of the 0.8 μm peak increases monotonously [Fig. 8(b)]. As is expected, the saturated intensity of the sample with C_{Er} of 0.07 at. % is much larger than that of the sample with C_{Er} of 0.02 at. %. It should be noted here that the PL intensity of the sample not containing nc-Si is much smaller than those containing nc-Si and saturation was not observed [Fig. 8(a)].

To further investigate the nc-Si mediated excitation mechanism of Er^{3+} , we also studied the excitation wavelength (λ_{ex}) dependence of the 1.54 and 0.8 μm peaks. Figure 9 shows the λ_{ex} dependence of the intensities of the 1.54 and 0.8 μm peaks for the sample with d_{Si} of 2.7 nm and C_{Er} of 0.11 at. %. For comparison purposes, the data for the sample not containing nc-Si is also shown (multiplied by a factor of 10). First, we compare the λ_{ex} dependence of the 1.54 μm peak with that of the 0.8 μm peak for the samples containing nc-Si and Er^{3+} . We can see that, as λ_{ex} increases, the intensities of the two peaks decrease almost monotonously, and the overall λ_{ex} dependence of the two peaks is very similar except for a dip at 488.0 nm for the 1.54 μm peak.

We now compare the λ_{ex} dependence of the 1.54 μm peak between the samples containing and not those containing nc-Si. We can see a completely different λ_{ex} dependence between the two samples. For the sample not containing nc-

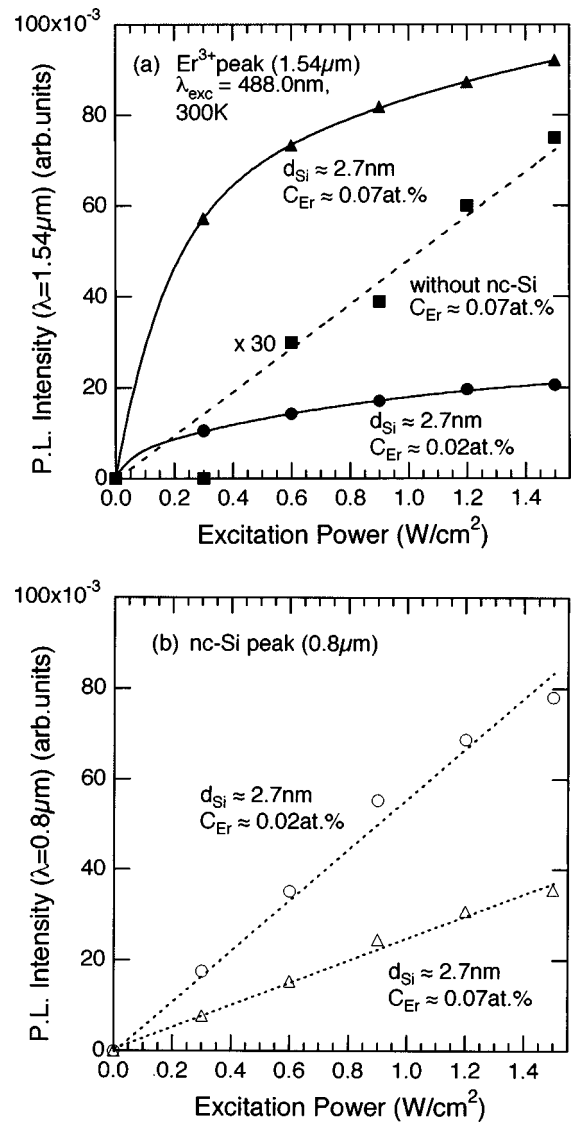


FIG. 8. PL intensities of (a) 1.54 and (b) 0.8 μm peaks as a function of excitation power for the samples with Er concentration of 0.02 and 0.07 at. %. The diameter of nc-Si for both the samples is about 2.7 nm. For comparison purposes, the PL intensity of the sample without nc-Si is also shown. The lines are drawn to guide the eye.

Si, the 1.54 μm PL was detectable only when the film was excited by 488.0 and 514.5 nm light, and no signal was detected with other λ_{ex} for the power density (1.5 W/cm^2) used in the experiment. The 488.0 and 514.5 nm correspond to the $^4I_{15/2} - ^4F_{7/2}$ and $^4I_{15/2} - ^2H_{11/2}$ transitions of Er^{3+} , respectively.² On the other hand, the sample containing nc-Si shows a dip at 488.0 nm. Although the origin of the dip is not clear at present, one possible explanation is as follows. At 488.0 nm excitation, Er^{3+} is excited both by the energy transfer from nc-Si and by the direct absorption of the excitation light. The direct absorption causes filling of the excited states, and thus the efficiency of the energy transfer may be reduced. This may result in a dip at the 488.0 nm excitation. The results of Fig. 9 clearly demonstrate that the excitation of Er^{3+} is not due to a direct absorption by Er^{3+} , but made by the energy transfer from nc-Si.

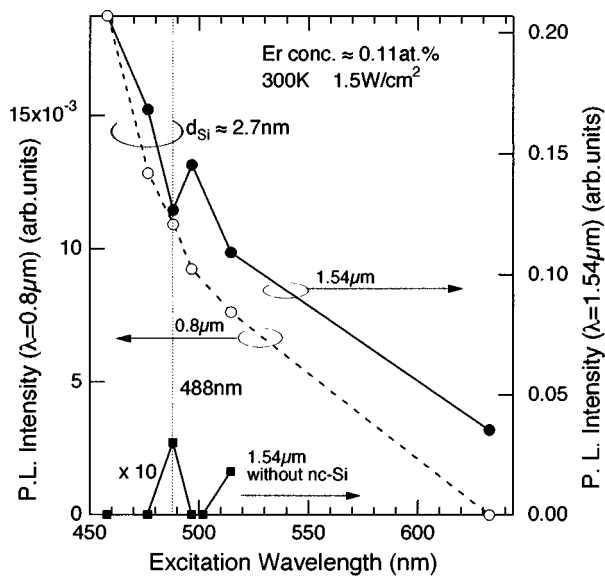


FIG. 9. PL intensities of 1.54 and 0.8 μm peaks as a function of excitation wavelength for samples with an Er concentration of 0.11 at. % and a nc-Si diameter of about 2.7 nm. For comparison purposes, the PL intensity of the sample without nc-Si is also shown.

As shown in Figs. 6 and 7, the thermal quenching of the 1.54 μm peak of the present samples is much smaller than that of the Er-doped bulk-Si crystal.⁴ In the case of the Er-doped bulk-Si crystal, the large thermal quenching is considered to be due to the increase in the probability of the phonon assisted back transfer of the energy from Er^{3+} to host Si crystals.⁴ In the present samples, the band gap of nc-Si is much larger than the bulk band gap, and thus the probability of the back transfer becomes much smaller because the back transfer requires multiple phonons. The band gap widening of nc-Si due to the quantum size effects is thus considered to be the primary cause of the small thermal quenching observed.

Similar small thermal quenching has been reported for Er-doped porous Si^{5,6,8} and semi-insulating polycrystalline silicon (SIPOS).⁴ The small quenching of Er-doped porous-Si is often explained in the same manner as that of the present samples, because it consists of nanometer-size Si grains.⁸ However, since porous Si is very complex in its structure and chemical components, PL mechanism of Er-doped porous Si is not fully understood. In particular, some authors claim that Er-related PL from Er-doped porous Si is not related to the quantum size effects in nc-Si but due to Er atoms incorporated into amorphous-Si:H:O regions in porous Si.^{5,6} In the case of SIPOS, a large band gap due to a high oxygen content (typically several tens of at. %) is considered to be the cause of the small quenching.⁵

A question arises as to whether the Er^{3+} responsible for the strong 1.54 μm PL is located inside or outside the nc-Si. Since the shape of the 1.54 μm peak depends on the local environment of Er^{3+} ,⁶ we compared the spectral shape of the samples containing nc-Si with that not containing nc-Si. Although the PL intensity became stronger by incorporating nc-Si, the spectral shape was almost identical for all the samples. This result and a relatively low solid solubility of

Er in Si ($\sim 10^{18}/\text{cm}^3$)²¹ suggest that the Er^{3+} responsible for the strong PL is around the interface region between nc-Si and SiO_2 , although a few Er^{3+} ions may exist in the nanocrystals.

V. CONCLUSION

We have studied PL properties of SiO_2 films containing nc-Si and Er. Peaks attributable to nc-Si (0.8 μm) and Er^{3+} (1.54 μm) were observed simultaneously. The correlation between the intensities of the two PL peaks was studied as a function of the size of nc-Si, Er concentration, excitation power and excitation wavelength. The most interesting result observed was that the 1.54 μm PL of Er^{3+} is strongly enhanced by incorporating nc-Si into the films, and the PL intensity depends on the size of nc-Si. Furthermore, we found that the intensity ratio of the 1.54 and 0.8 μm peaks is a constant independent of the size of nc-Si, provided that the Er concentration in the films is fixed. This implies that incorporation of "brighter" nanocrystals results in the stronger 1.54 μm PL. Since the nc-Si becomes "brighter" as the size decreases, the 1.54 μm PL will be more intense as the size of the nc-Si incorporated decreases. The 1.54 μm PL exhibited very small thermal quenching. The small thermal quenching is considered to be due to the widening of the band gap by the quantum size effects. Therefore, we can conclude that two major features of the quantum size effects of nc-Si, i.e., the band gap widening and the increases in the PL efficiency with decreasing the size, contribute to the improvement of room temperature PL efficiency of Er^{3+} .

ACKNOWLEDGMENT

This work was partially supported by a Grant-in-Aid for Scientific Research from the Ministry of Education, Science, Sports and Culture.

- ¹S. Coffa, F. Priolo, G. Franzo, V. Bellani, A. Carnera, and C. Spinella, *Phys. Rev. B* **48**, 11782 (1993).
- ²H. Przybylinska, W. Jantsch, Yu. Suprun-Bellevitch, M. Stepihova, L. Palmetshofer, G. Hendorfer, A. Kozanecki, R. J. Wilson, and B. J. Sealy, *Phys. Rev. B* **54**, 2532 (1996).
- ³J. Stimmer, A. Reittinger, J. F. Nützel, G. Abstreiter, H. Holzbrecher, and Ch. Buchal, *Appl. Phys. Lett.* **68**, 3290 (1996).
- ⁴G. N. van den Hoven, Jung H. Shin, A. Polman, S. Lombardo, and S. U. Campisano, *J. Appl. Phys.* **78**, 2642 (1995).
- ⁵A. Polman, *J. Appl. Phys.* **82**, 1 (1997).
- ⁶J. H. Shin, G. N. van den Hoven, and A. Polman, *Appl. Phys. Lett.* **66**, 2379 (1995).
- ⁷A. Dorofeev, E. Bachilo, V. Bondarenko, N. Gaponenko, N. Kazuchits, A. Leshok, G. Troyanova, N. Vorozov, V. Borisenko, H. Gnaser, W. Bock, P. Becker, and H. Oechsner, *Thin Solid Films* **276**, 171 (1996).
- ⁸U. Hömmerich, F. Namavar, A. Cremins, and K. L. Bray, *Appl. Phys. Lett.* **68**, 1951 (1996).
- ⁹X. Wu, U. Hömmerich, F. Namavar, and A. M. Cremins-Costa, *Appl. Phys. Lett.* **69**, 1903 (1996).
- ¹⁰Y. Kanzawa, T. Kageyama, S. Takeoka, M. Fujii, S. Hayashi, and K. Yamamoto, *Solid State Commun.* **102**, 533 (1997).
- ¹¹H. Takagi, H. Ogawa, Y. Yamazaki, A. Ishizaki, and T. Nakagiri, *Appl. Phys. Lett.* **56**, 2379 (1990).
- ¹²S. Schuppler, S. L. Friedman, M. A. Marcus, D. L. Adler, Y. H. Xie, F. M. Ross, Y. J. Chabal, T. D. Harris, L. E. Brus, W. L. Brown, E. E. Chaban, P. F. Szajowski, S. B. Christman, and P. H. Citrin, *Phys. Rev. B* **52**, 4910 (1995).
- ¹³Y. Kanzawa, M. Fujii, S. Hayashi, and K. Yamamoto, *Solid State Commun.* **100**, 227 (1996).

- ¹⁴M. Fujii, Y. Kanzawa, S. Hayashi, and K. Yamamoto, *Phys. Rev. B* **54**, 8373 (1996).
- ¹⁵M. Fujii, M. Yoshida, Y. Kanzawa, S. Hayashi, and K. Yamamoto, *Appl. Phys. Lett.* **71**, 1198 (1997).
- ¹⁶M. Fujii, S. Hayashi, and K. Yamamoto, *J. Appl. Phys.* **83**, 7953 (1998).
- ¹⁷B. Delley and E. F. Steigmeier, *Phys. Rev. B* **47**, 1397 (1993).
- ¹⁸L. E. Brus, P. F. Szajowski, W. L. Wilson, T. D. Harris, S. Schuppler, and P. H. Citrin, *J. Am. Chem. Soc.* **117**, 2915 (1995).
- ¹⁹S. Gardelis and B. Hamilton, *J. Appl. Phys.* **76**, 5327 (1994).
- ²⁰V. Petrova-Koch, T. Muschik, G. Polisski, and D. Kovalev, *Mater. Res. Soc. Symp. Proc.* **358**, 483 (1995).
- ²¹D. J. Eaglesham, J. Michel, E. A. Fitzgerald, D. C. Jacobson, J. M. Poate, J. L. Benton, A. Polman, Y. H. Xie, and L. C. Kimerling, *Appl. Phys. Lett.* **58**, 2797 (1991).